



Regioregular poly(3-hexylthiophene)-poly(ϵ -caprolactone) block copolymers: Controlled synthesis, microscopic morphology, and charge transport properties

Mathieu Surin^{a,c}, Olivier Coulembier^{b,c}, Khoa Tran^{b,c}, Julien De Winter^d, Philippe Leclère^{a,c}, Pascal Gerbaux^d, Roberto Lazzaroni^{a,c,*}, Philippe Dubois^{b,c,*}

^a Laboratory for Chemistry of Novel Materials, University of Mons – UMONS, 20, Place du Parc, 7000 Mons, Belgium

^b Laboratory of Polymeric and Composite Materials, University of Mons – UMONS, 20, Place du Parc, 7000 Mons, Belgium

^c Center for Innovation and Research in Materials and Polymers (CIRMAP), University of Mons – UMONS, 20, Place du Parc, 7000 Mons, Belgium

^d Mass Spectrometry Center, Laboratory of Organic Chemistry, University of Mons – UMONS, 20, Place du Parc, 7000 Mons, Belgium

ARTICLE INFO

Article history:

Received 12 October 2009

Received in revised form 12 January 2010

Accepted 17 January 2010

Available online 25 January 2010

Keywords:

GRIM polymerization

Poly(3-hexylthiophene)

Rod-coil copolymers

Atomic force microscopy

Organic field-effect transistors

ABSTRACT

In this paper, we describe the design and characterization of regioregular poly(3-hexylthiophene)-poly(ϵ -caprolactone) di- and tri-block copolymers (RRP3HT-*b*-PCL and PCL-*b*-RRP3HT-*b*-PCL). The well-controlled synthesis of (di)hydroxyl-terminated RRP3HT makes possible to design block copolymer structures with a narrow molecular weight distribution. The microscopic morphology is investigated by atomic force microscopy, which reveals self-assembled fibrillar structures with the RRP3HT nanoribbons separated by narrow domains of insulating PCL. The charge transport properties are characterized in thin films field-effect transistors, and comparison between the devices performances is carried out in view of the nanoscale morphology within the transistor channel.

© 2010 Elsevier B.V. All rights reserved.

1. Introduction

Regioregular poly(3-alkylthiophene)s (RRP3AT) [1] constitute a landmark as organic semiconductors because of their high charge carrier mobility in field-effect transistors (FET) [2,3] and their extensive use in the fabrication of organic photovoltaic diodes for solar cells applications (mostly in bulk heterojunction architectures with fullerene derivatives [4–8]). Recently, various copolymers containing a polythiophene segment have been designed in order to obtain novel materials combining good charge transport properties with superior or novel properties in terms of solubility or amphiphilic character, or compatibility with

molecules such as fullerene derivatives or carbon nanotubes [9–14]. In this context, combining a (semi-)rigid RRP3AT block with insulating flexible block(s) could yield interesting materials, often referred to as “rod-coil” block copolymers. This type of copolymers can generate unique solid-state morphologies resulting from the nanoscale phase-separation of the different blocks, and could lead to tailored electronic and photonic materials [15–20]. This “rod-coil” block copolymer approach has been recently exploited by McCullough et al., who designed structures containing a regioregular poly(3-hexylthiophene) (RRP3HT) segment copolymerized with styrene or various methacrylate-based monomers (thanks to the control over the end-groups of RRP3HT), and correlated the nanoscale ordering within copolymers films with their electrical conductivity [21,22]. A variety of other block copolymer structures have been obtained by association of the living Grignard metathesis (GRIM) process of halogeno-functionalized 3-hexylthiophene monomers with atom-transfer radical,

* Corresponding authors. Address: Center for Innovation and Research in Materials and Polymers (CIRMAP), Laboratory of Polymeric and Composite Materials, University of Mons – UMONS, 20, Place du Parc, 7000 Mons, Belgium.

E-mail addresses: roberto.lazzaroni@umons.ac.be (R. Lazzaroni), philippe.dubois@umons.ac.be (P. Dubois).

ring-opening metathesis, reversible addition fragmentation chain transfer and nitroxide mediated polymerizations [22–26]. Recently, the GRIM approach has been associated with the ring-opening polymerization (ROP) of D,L-lactide [27]. Extending this family of block copolymers with other lactones would yield interesting materials, especially by polymerizing ϵ -caprolactone (CL) onto RRP3HT segment since poly(ϵ -caprolactone) (PCL) is: (1) crystallizable (in contrast to other segments copolymerized with P3HT, such as poly(methacrylate)s [22]); (2) miscible with a number of other polymer compounds (such as poly(vinyl chloride), poly(ethylene chloride), poly(styrene-co-acrylonitrile),...); (3) removable by hydrolysis, and; (4) biocompatible. The capacity of PCL to be miscible blended with various commercial polymers over a wide range of composition (in contrast to polylactide blocks) opens the way for interesting compatibilization of a P3HT matrix by using P3HT/PCL block copolymers, whatever their topology. PCL is therefore a valuable partner for RRP3HT for improved compatibility and for potential bio-applications.

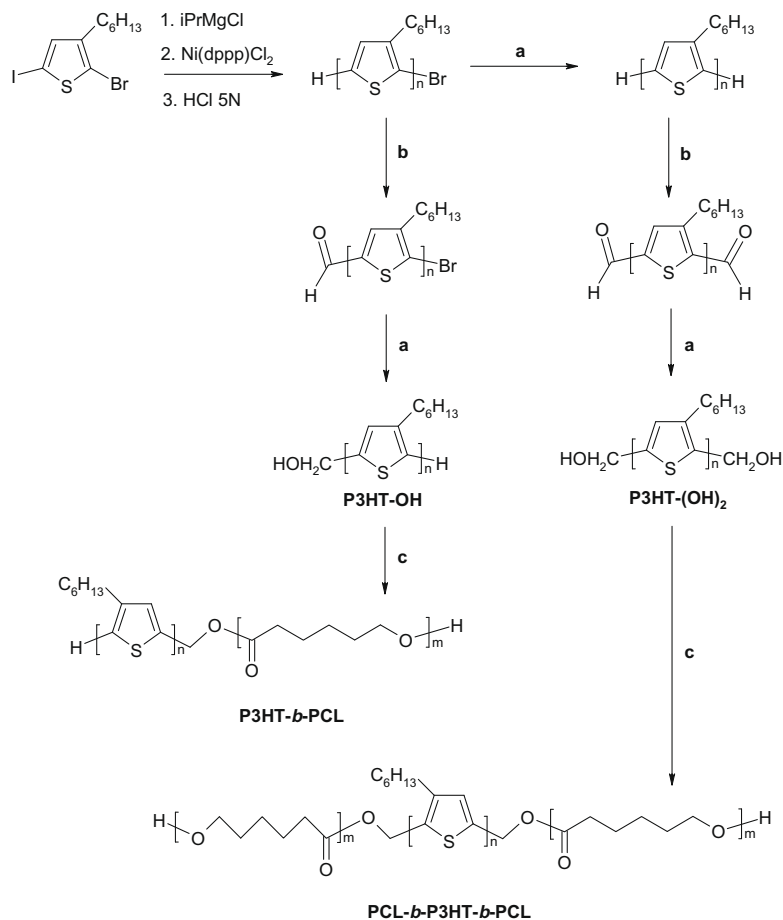
Here, we report on the stepwise synthesis of diblock and triblock copolymers by controlled polymerization of ϵ -caprolactone from (di)hydroxyl-terminated RRP3HT, see Scheme 1. Such copolymers are inherently expected

to self-assemble in the solid-state; the resulting nanoscale morphologies in thin deposits are studied via atomic force microscopy (AFM) and correlated with the charge transport properties in field-effect transistor configuration.

2. Experimental section

2.1. Synthesis

α -bromo poly(3-hexylthiophene): Into a flask under a nitrogen atmosphere containing 2-bromo-3-hexyl-5-iodothiophene (1.18 g, 3.15 mmol), dry THF (15.0 mL) was added via a syringe, and the mixture was stirred at 0 °C. *i*-PrMgCl (2.0 M solution in THF, 1.08 mL, 3.15 mmol) was added via a syringe, and the mixture was stirred at 0 °C for 0.5 h. A suspension of Ni(dppp)Cl₂ (18 mg, 0.03 mmol) in THF (5.0 mL) was added to the mixture via a syringe at 0 °C, and then the mixture was stirred at room temperature. After the reaction mixture was stirred for 1 day, a 5 N HCl aqueous solution was quickly added to quench the reaction. The mixture was stirred for 0.5 h more, then precipitated in cold MeOH. The product was washed with MeOH yielding a purple solid, >98.5% rr-HT-P3HT. Yield = 69%; UV (CHCl₃, nm): 445; IR (cm⁻¹): 819 (C–H



Scheme 1. Comparative routes leading to diblock (P3HT-*b*-PCL) and triblock (PCL-*b*-P3HT-*b*-PCL) copolymers. Reagents a: LiAlH₄/HCl, b: 1. POCl₃/DMF, 2. CH₃COONa/H₂O, and c: CL/SnOct₂.

aromatic out-of-plane) and $I_{\text{sym}}/I_{\text{asym}} = 6$, characteristic of rr-HT-P3HT; $^1\text{H NMR}$ (300 Hz, CDCl_3): 6.98 (s, 1H), 2.80 (t, $^3J = 7.5$ Hz, 2H), 1.71 (quint, 2H), 1.34 (m, 6H), 0.91 (t, $^3J = 6.4$ Hz, 3H); GPC analysis: $M_n = 4450$ g/mol; PDI = 1.17. **Formyl-de-hydrogenation of α -bromo poly(3-hexylthiophene)**: H-P3HT-Br ($M_n = 3700$, PDI = 1.17) (300 mg, 0.071 mmol) was dissolved in anhydrous toluene (80 mL) under N_2 . N,N-Dimethylformamide (1 mL, 13 mmol) and POCl_3 (0.7 mL, 7.6 mmol) were added. The reaction was carried out first at 75 °C for 50 h. The solution was cooled down to room temperature, followed by the adding of a saturated aqueous sodium acetate solution. The reaction mixture was stirred for another 2 h. The polymer was precipitated in cold methanol and washed with water, then methanol. Yield = 94%; GPC analysis: $M_n = 4800$ g/mol; PDI = 1.17; $^1\text{H NMR}$ (300 Hz, CDCl_3): $M_n\text{NMR} = 5400$ g/mol. **Reduction of α -bromo, ω -formyl poly(3-hexylthiophene)**: HOC-P3HT-Br ($M_n = 3500$, PDI = 1.23; 200 mg, 0.057 mmol) was dissolved in anhydrous THF (80 mL), under N_2 . LiAlH_4 1 M solution in THF (0.5 mL) was then added. The reaction was then kept stirring at room temperature for 1.5 h. HCl (1 N, 1 mL) was then added to quench the excess of LiAlH_4 . The polymer was precipitated in methanol and washed with water then methanol. After drying in vacuum, 190 mg of CH_2OH -P3HT-Br was obtained. Yield = 95%; GPC analysis: $M_n = 5100$ g/mol; PDI = 1.22; $^1\text{H NMR}$ (300 Hz, CDCl_3): $M_n\text{NMR} = 5400$ g/mol. **Synthesis of poly(3-hexylthiophene)-*b*-poly(ϵ -caprolactone)**: In a previously dried and nitrogen-purged 25 mL round-bottom flask equipped with a three-way stopcock and a rubber septum, 0.43 mL of CL (3.92 mmol) and 3.3 mL of dried toluene were added to freshly dried 0.5 g of hydroxyl-P3HT (0.098 mmol). The reaction mixture was gently heated to 110 °C until complete dissolution of P3HT before adding a 0.2 M solution of $\text{Sn}(\text{Oct})_2$ (0.2 mL, 0.039 mmol, $[\text{OH}]_0/[\text{Sn}(\text{Oct})_2]_0 = 2.5$, final concentration of CL = 1 M). After 15 h at 110 °C, the reaction was cooled down and stopped by adding dropwise an aqueous HCl solution (1 mol L^{-1}). The copolymer was then precipitated from cold methanol yielding a brown solid. Yield = 76% ($m = 704$ mg); $^1\text{H NMR}$ (300 Hz, CDCl_3): $M_n\text{PCL} = 2300$ g/mol; Conversion in PCL = 50.4% (M_n in PCL expected = $40 \times 114 = 4560$ g/mol); GPC analysis: $M_n\text{GPC} = 6500$ g/mol; PDI = 1.23. A detailed description of the materials, synthesis steps and characterization techniques is given in the Supporting information.

2.2. Atomic force microscopy

Sub-monolayer deposits were prepared by solvent casting on freshly-cleaved muscovite mica or silicon oxide substrates from dilute solutions (0.05–0.5 g L^{-1}); the solvent was slowly evaporated at room temperature in a solvent-saturated atmosphere. Thicker, homogeneous films were prepared by spin-coating the solutions onto silicon oxide or glass substrates (spinning speed from 2500 to 4000 rpm, solution concentration = 1.0 g L^{-1}). AFM studies were carried out in Tapping-Mode with Multimode Nanoscope IIIa or Nanoscope V microscopes (Veeco) operating in air at room temperature, using microfabricated silicon cantilevers with a spring constant of around 30 N m^{-1}

(TESP, Veeco). Images of different areas of the samples were collected and Nanoscope image processing software was used for image analysis.

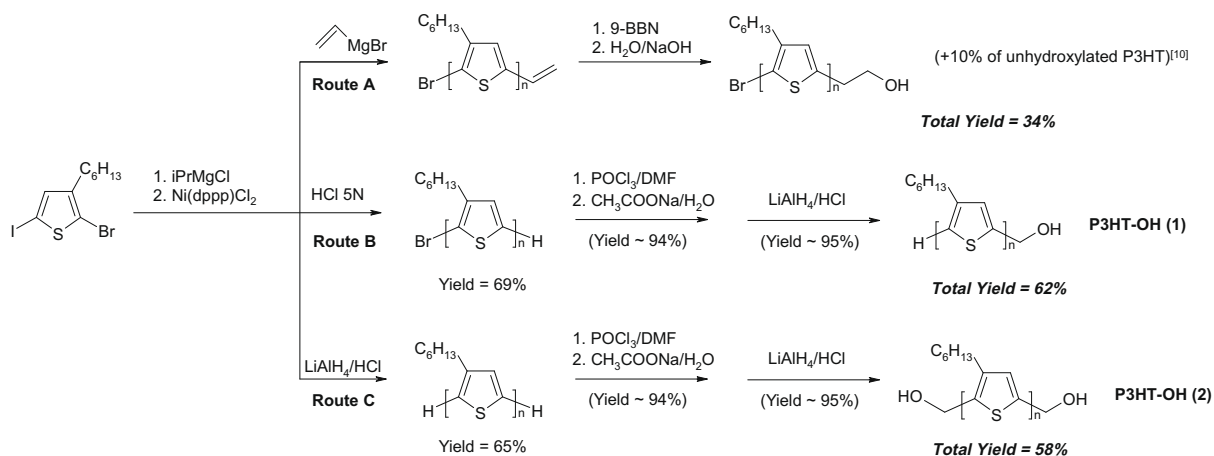
2.3. FET fabrication and characterization

The FET devices consist in a thermally-grown 200 nm-thick SiO_2 gate dielectric on top of a doped n^{++} -type Si gate electrode. Gold source and drain electrodes were used, and the devices were fabricated either in bottom-contact (100 nm-thick electrodes, channel length of 5 or 10 μm) or top-contact (channel length of 50 μm) configurations. Homogeneous thin films of the (co)polymers were prepared by spin-coating a 1.0 g L^{-1} solution (at 2500 rpm) onto the silicon oxide gate dielectrics. The devices were then tested in a glove box under nitrogen atmosphere and the electrical characteristics were measured on a probe station with a Keithley 4200 semiconductor parametric analyzer. The charge mobility has been estimated from the saturation regime (at source-drain voltage of -60 V), see the description in Refs. [35,40–44] for instance.

3. Results and discussion

3.1. Synthesis of (co)polymers

The key-step for the controlled generation of these novel architectures is the synthesis of perfectly controlled (di)hydroxyl-terminated regioregular P3HT. The first method considered for the synthesis of P3HT-OH consisted in the hydroboration/oxidation reaction of previously synthesized vinyl-terminated P3HT, as recently reported by McCullough et al. (Route A, Scheme 2) [28]. However, the expected P3HT-OH compound was systematically contaminated by ca. 10 wt.% of non-hydroxylated P3HT [23,29] (see Supporting information, SI) leading upon ring-opening polymerization of ϵ -caprolactone (CL) to a mixture of P3HT-*b*-PCL and P3HT and requiring intensive purification by fractionation. Comparatively, the formyl-dehydrogenation of the α -bromo P3HT protic end-group (Route B) was successfully performed by a Vilsmeier reaction leading to α -bromo, ω -formyl P3HT characterized by a recovering yield of 94% [23,29]. The evolution of the reaction was followed by MALDI-ToF analysis until complete transformation of the α -bromo P3HT to α -bromo, ω -formyl P3HT (Fig. S2) allowing us to recover a 100% formyl end-capped structure. After completion of the reaction, both the formyl and the bromide end-groups were reduced by LiAlH_4 yielding the expected P3HT-OH with a narrow molecular weight distribution (polydispersity index = 1.22) and a recovering yield of 95% (see SI, Fig. S3). It is worth noting that the global yield of the polymerization and the post-polymerization end-group modification processes reached 62%. Such a high yield, together with the fact that the recovered P3HT-OH is 100% functionalized by a hydroxyl group, represents a relevant progress in the field. Dihydroxyl-terminated P3HT (P3HT-(OH) $_2$) was also obtained by the same procedure but starting with a reduction reaction of α -bromo P3HT by LiAlH_4 (Total recovering yield: 58%,



Scheme 2. Comparative routes leading to (di)hydroxyl-terminated P3HT. Route A: hydroboration/oxidation of α -bromo, ω -vinyl P3HT [10]. Routes B and C: vilsmeier oxidation/reduction of (α -bromo) P3HT.

Route C, Scheme 2, Fig. S4). The molecular characterization of representative P3HT is described in Table 1.

These homopolymers were used as the starting materials for the synthesis of di- and triblock copolymers shown in Scheme 1. Tin(II)octoate ($\text{Sn}(\text{Oct})_2$) was used to catalyze the controlled ROP of CL from the hydroxyl-end-groups(s) of P3HT macroinitiators [30]. Both P3HT-OH and P3HT-(OH)₂ were thus treated with $\text{Sn}(\text{Oct})_2$ in toluene with an initial hydroxyl/Sn molar ratio of 2.5. CL was then added and the polymerization was carried out in toluene at 110 °C with an initial monomer concentration of 1 M and an initial $[\text{CL}]_0/[\text{OH}]_0$ molar ratio of 40. After a reaction time of 15 h, the copolymers were recovered by precipitation (see SI); the PCL molecular weights (M_n), as estimated from ¹H NMR, are 1900 and 3200 g/mol for P3HT-*b*-PCL and PCL-*b*-P3HT-*b*-PCL, respectively (Table 1). These values are in good agreement with the expected molecular weights taking into account the monomer conversion and initial monomer-to-initiator molar ratios. Size exclusion chromatography traces of the copolymers were all monomodal with polydispersity indices below 1.2 (Table 1 and SI).

3.2. Microscopic morphology in thin deposits

The micro- and nano-scopic morphology of thin deposits of the (co)polymers was investigated by atomic force microscopy (AFM) in intermittent-contact mode. Thin

deposits have been prepared by drop-casting or spin-coating onto various substrates starting from good solvents for both P3HT and PCL blocks (e.g., tetrahydrofuran, toluene or chlorobenzene). Thin deposits of the studied compounds all show a fibrillar (nanowire-like) morphology (see AFM images in Fig. 1). This is observed for both sub-monolayer deposits (Fig. 1c and Fig. 1e, where the substrate surface appears dark) and for thicker deposits (Fig. 1a,b,d) prepared by drop-casting, in which the fibrils extend up to a few μm and arrange in lamellae. Films prepared by spin-coating from the same solvent (tetrahydrofuran) also show entangled fibrillar structures (Fig. 1f), indicative that the fibrillar assembly occurs even with a very rapid solvent evaporation process (spinning speed >2500 rpm). Indeed, this fibrillar morphology is typical from the (crystalline) assembly of RRP3HT into π -stacked assemblies, as observed and described for highly regioregular poly(thiophene)s and other conjugated (co)polymers thin deposits prepared with the same methods [31,32]. In these fibrils, P3HT molecules have extended conjugated backbones, with their long axis perpendicular to the π -stacking direction (the fibril axis). The fibrils arrange in lamellae due to interdigitation of alkyl groups perpendicularly to the backbone axis with a lamellar thickness of 1.7 nm, as observed using (Grazing Incidence) X-ray Diffraction measurements [33–34], which is in agreement with the fibril thickness measured here. This is further supported by the measured width of the fibrils, which

Table 1

Molecular characteristics and FET properties of the synthesized RRP3HT and their corresponding PCL-based copolymers.

Compound	M_n P3HT (g/mol) ^a	M_n PCL (g/mol) ^a	M_n GPC (g/mol) ^b	PDI ^b	μ^d (cm ² V ⁻¹ s ⁻¹)	$I_{\text{on/off}}^d$
P3HT-OH	5400 ^c	–	5100	1.22	–	–
P3HT- <i>b</i> -PCL	6000	1900	6500	1.23	1.1×10^{-5}	$\sim 1 \times 10^3$
P3HT-(OH) ₂	7400 ^c	–	8700	1.16	6.0×10^{-5}	$\sim 3 \times 10^3$
PCL- <i>b</i> -P3HT- <i>b</i> -PCL	7900	3200	12100	1.15	4.6×10^{-4}	$\sim 2 \times 10^4$

^a Absolute molar masses as determined by ¹H NMR analysis.

^b Relative molar masses as determined by gel permeation chromatography in THF at 35 °C using PS standards.

^c Molar masses obtained by ¹H NMR analysis have been calculated after confirmation of the number of hydroxyl-end-groups by MALDI-Tof.

^d Charge mobilities μ and current on/off ratios $I_{\text{on/off}}$ have been estimated from the transfer characteristics of top-contact FET devices.

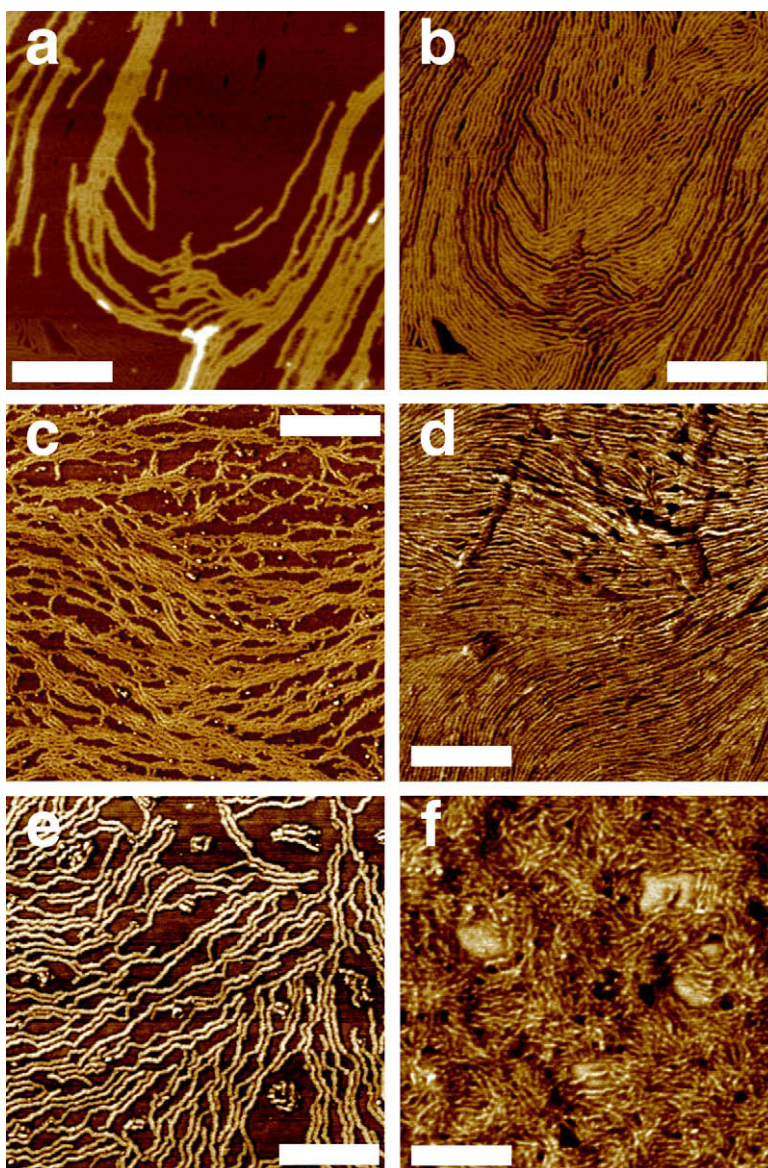


Fig. 1. AFM images of thin deposits from tetrahydrofuran of (a–b) P3HT-OH (a: height; b: phase); (c–d) P3HT-*b*-PCL (phase images, c: sub-monolayer deposit; d: thick film); (e–f) PCL-*b*-P3HT-*b*-PCL (phase images, e: sub-monolayer deposit; f: spin-coated film). The white scale bar is 250 nm-long.

correlates with the length of the P3HT conjugated backbone [35]: the measured widths are 11 ± 2 nm for P3HT-OH and 17 ± 2 nm for PCL-*b*-P3HT-*b*-PCL, while the estimated lengths of fully-extended P3HT backbones are 12.6 and 18.4 nm in average, respectively [36]. Note that, for the P3HT-*b*-PCL and PCL-*b*-P3HT-*b*-PCL block copolymers, adjacent fibrils (in bright) are close to each other, and appear to be separated by narrow dark bands in the phase images (for instance, compare Fig. 1b and Fig. 1e). This, together with the fact that the measured fibrils width is close to the length of the extended P3HT backbone, indicates that the PCL segments are very likely in a compact conformation in between the P3HT assemblies. Indeed, the PCL segments have a quite low degree of

polymerization in these block copolymer structures (e.g. 20 monomer units in average in the diblock copolymer), which seems not sufficient to induce crystallization of PCL. If we consider a coiled conformation of the PCL segments, the estimated radius of gyration would be around 1.3–1.6 nm (in the di- and tri-block copolymers), i.e. around 3 nm in diameter [36]. All these results suggest that the self-assembly of these block copolymers is driven by the ordering of the RRP3HT backbones (intra-lamellar π -stacking of conjugated backbones and inter-lamellar interdigitation between alkyl groups) rather than by the assembly of the PCL segments, which are very likely in a coiled configuration in between the P3HT fibrils [37].

3.3. Charge transport properties in field-effect transistors

Field-effect transistors (FET) were fabricated in bottom-gate configuration, with a gate dielectric layer made of SiO₂ on top of a heavily doped silicon (*n*⁺) gate electrode. Thin films of the (co)polymers were deposited by spin-coating on the SiO₂ from chlorobenzene solutions because this deposition process leads to flat, homogeneous thin films suitable for FET fabrication (thickness $\sim 20 \pm 5$ nm and RMS roughness (over 1 μm^2) of about 2 nm, as measured with AFM). The devices were tested with gold source and drain electrodes either in top-contact or bottom-contact configurations, in the accumulation regime of hole transport (negative source-gate voltages) since holes are the major charge carriers in P3HT structures using this device architecture. Here we report results for top-contact FET devices, which show more reproducible FET characteristics using these preparation conditions [38]. Examples of transfer and output characteristics are shown in Fig. 2. For all (co)polymers, the output characteristics (source-drain current I_{ds} versus source-drain voltage V_{ds} at various gate voltages V_{gs}) show good saturation behavior, and the curves display typical characteristics of P3HT films using this preparation method [2,39]. From the transfer characteristics, we observe that the threshold voltages are close to 0 V, and the current on/off ratios are on the order of 10^3 – 10^4 (see Table 1). All these results show that the studied compounds behave as semiconducting polymers with

low level of doping. The charge carrier mobilities μ , estimated in the saturation regime (i.e., from the slope of the plot of I_{ds} versus $V_{\text{gs}}^{1/2}$ at source-drain voltage $V_{\text{ds}} = -60$ V), are listed in Table 1. The μ values are in the range of 10^{-5} – 10^{-3} $\text{cm}^2 \text{V}^{-1} \text{s}^{-1}$; this is quite low compared to the highest mobilities reported for polymer FETs, which are on the order of 0.1–1 $\text{cm}^2 \text{V}^{-1} \text{s}^{-1}$ for thiophene-based or thienothiophene-based polymers [40–42]. This difference can be attributed to the low molecular weight of the P3HT-based polymers studied here (maximum 7600 g/mol, corresponding to about 46 hexylthiophene units). Indeed, it has been shown that FETs made of low molecular weight fractions of P3HT show lower charge carrier mobilities: for $M_n < 10000$ g/mol, the charge mobility estimated in the same manner is $\sim 10^{-5}$ – 10^{-4} $\text{cm}^2 \text{V}^{-1} \text{s}^{-1}$. For higher molecular weight fractions (10000 g/mol $< M_n < 40000$ g/mol), μ is up to 10^{-2} $\text{cm}^2 \text{V}^{-1} \text{s}^{-1}$. This difference has been attributed to the existence of charge transport pathways along longer chains connecting crystalline domains in the film and/or the more planar conformations in films of high molecular weight RRP3HT [43–44]. Surprisingly, we observe that the triblock copolymer film displays the highest value (around 0.5×10^{-3} $\text{cm}^2 \text{V}^{-1} \text{s}^{-1}$), i.e. one order of magnitude higher than that of the corresponding P3HT homopolymer (0.6×10^{-4} $\text{cm}^2 \text{V}^{-1} \text{s}^{-1}$) despite the fact that P3HT represents only about 60% by weight. This difference is not related to a molecular weight difference of the P3HT sequence, see Table 1. In our interpretation, it origi-

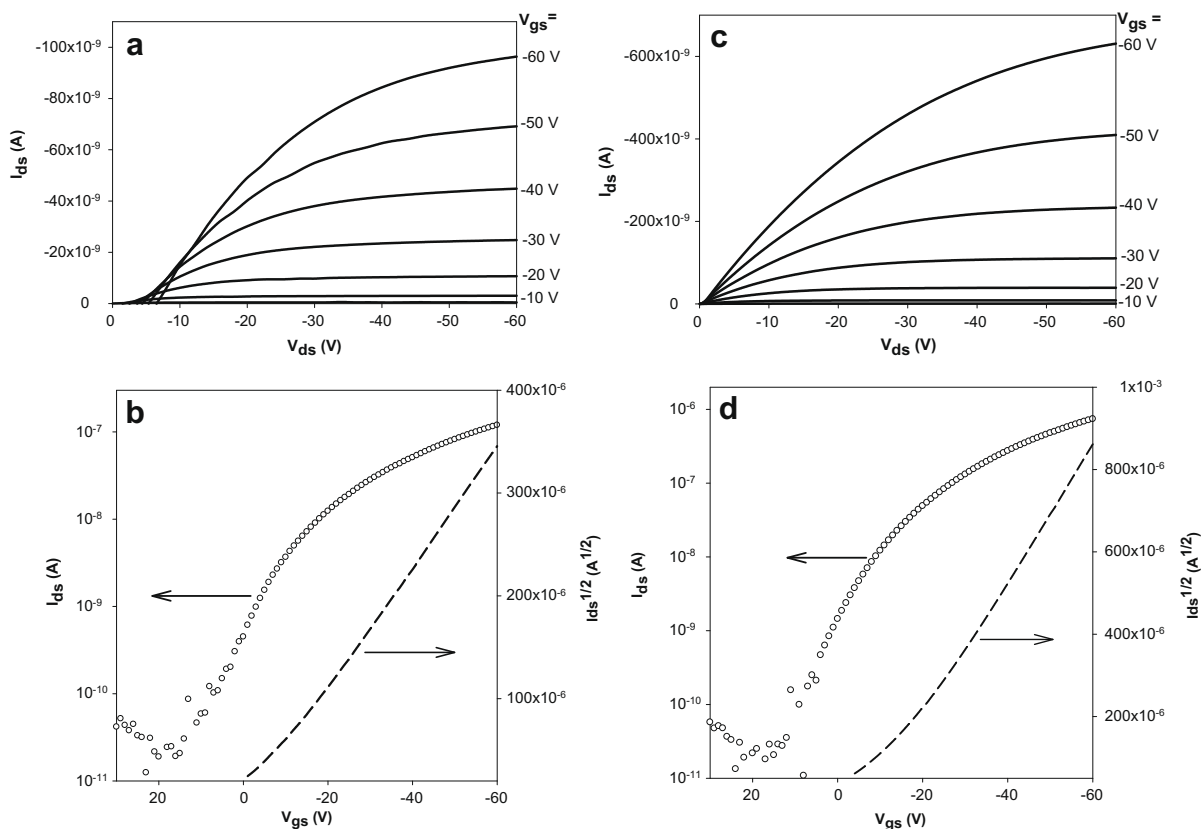


Fig. 2. Output (top) and transfer (bottom) characteristics of top-contact FET devices made of P3HT-(OH)₂ (a,b) and PCL-*b*-P3HT-*b*-PCL (c,d) as active layers.

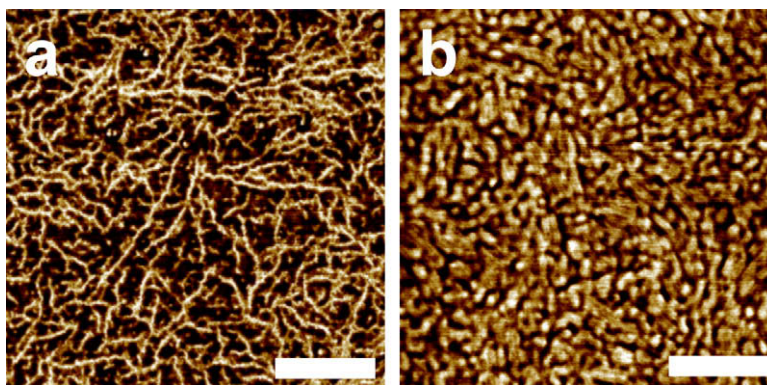


Fig. 3. AFM phase images of the active layer within the FET channel of (a) PCL-*b*-P3HT-*b*-PCL, and (b) P3HT-(OH)₂. The white scale bar is 250 nm-long.

nates from a difference in structural order within the thin films and/or interface with the electrodes. AFM measurements on the active layer in the channel of FET devices (see Fig. 3) reveal that films of PCL-*b*-P3HT-*b*-PCL show a higher degree of fibrillar order than pure P3HT-(OH)₂. The fibrils are relatively long in the case of PCL-*b*-P3HT-*b*-PCL (few hundreds nm-long) compared to the assemblies of P3HT-(OH)₂, which are confined in tens of nm-wide granular domains. In FET devices made of pure RRP3HT, it has been shown that films made of μm -long fibrillar structures lead to higher performances (i.e., charge mobility and current on/off ratio) than untextured, non-crystallized films, demonstrating that the fibrils act as efficient “conduits” for the charge transport in FET (in which the channel length is typically a few μm -long) [33]b,[35,39]. The higher degree of fibrillar order in PCL-*b*-P3HT-*b*-PCL spin-coated films is likely due to the tendency of this copolymer to phase-separate on the nanoscale, which probably forces the P3HT segments to be more in registry with each other and therefore leads to straight and long P3HT fibrils separated by small PCL domains. The higher charge carrier mobility observed here for the triblock copolymer also suggests that the charge transport is one-dimensional (along each fibril) rather than inter-fibrillar (bi-dimensional) in these materials [45], since in the case of the triblock copolymer film, the P3HT fibrils are surrounded by the PCL segments on each side, which are likely to insulate the π -conjugated systems of adjacent fibrils from each other.

4. Conclusions

In summary, we have described a well-controlled synthesis method for the design of poly(thiophene) block copolymers. Each reaction step has been carefully followed, making it possible to recover the target compounds in high yields without tedious purification steps. Regioregular P3HT homopolymers and P3HT-PCL block copolymers self-assemble into well-defined fibrillar structures. The charge transport properties of these (co)polymers have been characterized in FETs, showing characteristics of good quality organic semiconductors, with charge carrier mobilities in the range of 10^{-5} – 10^{-3} $\text{cm}^2 \text{V}^{-1} \text{s}^{-1}$. Interestingly, the copolymer PCL-*b*-P3HT-*b*-PCL shows higher charge

mobility than the corresponding pure P3HT block, which is attributed to a higher degree of long-range fibrillar structures favored by nanophase separation. Since P3HT can be chemically doped after the self-assembly process and the lateral dimensions can be tuned by controlled synthesis of the polymer segments, these copolymers could be suitable materials for fabricating conducting nanowires insulated from each other. Moreover, the possibility of removing the PCL segments by hydrolysis shows potential for designing nano-sized pores (in between RRP3HT segments) [27] that could then be filled with electron acceptor molecules, which would be of interest for designing organic photovoltaic diodes with improved performances thanks to fine-control over the nanoscale morphology.

Acknowledgments

The authors thank the financial support from the Walloon Region, the European Commission (FSE, FEDER), the National Fund for Scientific Research (F.R.S.-FNRS), and the Belgian Federal Science Policy Office (PAI 6/27). J.D. is Research Fellow and M.S., O.C, Ph.L., P.G. are Research Associates of the F.R.S.-FNRS. M.S. thanks Prof. Alan J. Heeger for a research stay in his group at University of California Santa Barbara and Drs. Jonathan D. Yuen, Shinuk Cho, and Daniel Moses for their kind help and enlightening discussions.

Supporting Information. Details of the synthesis and characterization are available from the authors or online on <http://www.sciencedirect.com>.

Appendix A. Supplementary data

Supplementary data associated with this article can be found, in the online version, at doi:10.1016/j.orgel.2010.01.016.

References

- [1] I. Osaka, R.D. McCullough, *Acc. Chem. Res.* 41 (2008) 1202.
- [2] (a) Z. Bao, A. Dodabalapur, A.J. Lovinger, *Appl. Phys. Lett.* 69 (1996) 4108;
(b) Z. Bao, A.J. Lovinger, *Chem. Mater.* 11 (1999) 2607.
- [3] (a) H. Sirringhaus, P.J. Brown, R.H. Friend, M.M. Nielsen, K. Bechgaard, B.M.W. Langeveld-Voss, A.J.H. Spiering, R.A.J. Janssen,

- E.W. Meijer, P. Herwig, D.M. de Leeuw, Nature 401 (1999) 685;
(b) A. Facchetti, Mater. Today 10 (2007) 28.
- [4] W.L. Ma, C.Y. Yang, X. Gong, K. Lee, A.J. Heeger, Adv. Funct. Mater. 15 (2005) 1617.
- [5] Y. Kim, S. Cook, S.M. Tuladhar, S.A. Choulis, J. Nelson, J.R. Durrant, D.D.C. Bradley, M. Giles, I. McCulloch, C.S. Ha, M. Ree, Nat. Mater. 5 (2006) 197.
- [6] J.Y. Kim, K. Lee, N.E. Coates, D. Moses, T.Q. Nguyen, M. Dante, A.J. Heeger, Science 317 (2007) 222.
- [7] S. Gunes, H. Neugebauer, N.S. Sariciftci, Chem. Rev. 107 (2007) 1324.
- [8] A.C. Mayer, S.R. Scully, B.E. Hardin, M.W. Rowell, M.D. McGehee, Mater. Today 10 (2007) 28.
- [9] K. Sivula, Z.T. Ball, N. Watanabe, J.M.J. Fréchet, Adv. Mater. 18 (2006) 206.
- [10] S.P. Economopoulos, C.L. Chochos, V.G. Gregoriou, J.K. Kallitsis, S. Barrau, G. Hadziioannou, Macromolecules 40 (2007) 921.
- [11] J.H. Zou, L.W. Liu, H. Chen, S.I. Khondaker, R.D. McCullough, Q. Huo, L. Zhai, Adv. Mater. 20 (2008) 2055.
- [12] Z.Y. Zhou, X.W. Chen, S.J. Holdcroft, Am. Chem. Soc. 130 (2008) 11711.
- [13] F. Ouhib, A. Khoukh, J.B. Ledeuil, H. Martinez, J. Desbrieres, C. Dagron-Lartigau, Macromolecules 41 (2008) 9736.
- [14] C.R. Craley, R. Zhang, T. Kowalewski, R.D. McCullough, M.C. Stefan, Macromol. Rapid Commun. 30 (2009) 11.
- [15] S.A. Jenekhe, X.L. Chen, Science 283 (1999) 372.
- [16] H.-A. Klok, S. Lecommandoux, Adv. Mater. 13 (2001) 1217.
- [17] M. Lee, B.-K. Cho, W.-C. Zin, Chem. Rev. (2001) 101.
- [18] D.M. Vriezema, J. Hoogboom, K. Velonia, K. Takazawa, P.C.M. Christianen, J.C. Maan, A.E. Rowan, R.J.M. Nolte, Angew. Chem., Int. Ed. 42 (2003) 772.
- [19] B.W. Messmore, J.F. Hulvat, E.D. Sone, S.I.J. Stupp, Am. Chem. Soc. 126 (2004) 14452.
- [20] B.D. Olsen, R.A. Segalman, Mater. Sci. & Eng. R-Reports 62 (2008) 37.
- [21] J.S. Liu, E. Sheina, T. Kowalewski, R.D. McCullough, Angew. Chem., Int. Ed. 41 (2001) 329.
- [22] M.C. Iovu, R. Zhang, J.R. Cooper, D.M. Smilgies, A.E. Javier, E.E. Sheina, T. Kowalewski, R.D. McCullough, Macromol. Rapid Commun. 28 (2007) 1816.
- [23] M.C. Iovu, M. Jeffries-El, E.E. Sheina, J.R. Cooper, R.D. McCullough, Polymer 46 (2005) 8582.
- [24] M.C. Iovu, E.E. Sheina, R.R. Gil, R.D. McCullough, Macromolecules 38 (2005) 8649.
- [25] M.C. Iovu, C.R. Craley, M. Jeffries-El, A.B. Krankowski, R. Zhang, T. Kowalewski, R.D. McCullough, Macromolecules 40 (2007) 4733.
- [26] G. Sauvé, R.D. McCullough, Adv. Mater. 19 (2007) 1822.
- [27] B. Boudouris, W.C.D. Frisbie, M.A. Hillmyer, Macromolecules 41 (2008) 67.
- [28] M. Jeffries-El, G. Sauvé, R.D. McCullough, Macromolecules 38 (2005) 10346.
- [29] J.S. Liu, R.D. McCullough, Macromolecules 35 (2002) 9882.
- [30] A. Duda, S. Penczek, A. Kowalski, J. Libiszowski, Macromol. Symp. 153 (2000) 41.
- [31] Ph. Leclère, M. Surin, P. Brocorens, M. Cavallini, F. Biscarini, R. Lazzaroni, Mater. Sci. & Eng. R-Reports 55 (2006) 1.
- [32] F.J.M. Hoebein, P. Jonkheijm, E.W. Meijer, A.P.H.J. Schenning, Chem. Rev. 105 (2005) 1491.
- [33] (a) J.A. Merlo, C.D.J. Frisbie, Phys. Chem. B 108 (2004) 19169;
(b) J.A. Merlo, C.D.J. Frisbie, Polym. Sci. B 41 (2003) 2674.
- [34] (a) S. Hugger, R. Thomann, T. Heinzl, T. Thurn-Albrecht, Colloid Polym. Sci. 282 (2004) 932;
(b) H.C. Yang, S. Park, D. Kim, K. Oh, S. Magonov, K. Cho, T. Chang, Z. Bao, C.Y. Ryu, Polym. Prepr. 44 (2003) 333;
(c) H. Yang, T.J. Shin, L. Yang, K. Cho, C.Y. Ryu, Z. Bao, Adv. Funct. Mater. 15 (2005) 671;
(d) H.C. Yang, T.J. Shin, Z. Bao, C.Y. Ryu, J. Polym. Sci., Part B: Polym. Phys. 45 (2007) 1303.
- [35] (a) M. Surin, Ph. Leclère, R. Lazzaroni, J.D. Yuen, G. Wang, D. Moses, A.J. Heeger, S. Cho, K. Lee, J. Appl. Phys. 100 (2006) 33712;
(b) S. Cho, K. Lee, J.D. Yuen, G. Wang, D. Moses, A.J. Heeger, M. Surin, R. Lazzaroni, J. Appl. Phys. 100 (2006) 33712.
- [36] The fully-extended length of RRP3HT chains is estimated by multiplying the average degree of polymerization N by the length of a monomer unit l (0.387 nm), taking into account the head-to-tail linkage of RRP3HT. The radius of gyration of the PCL coil is estimated with $R_g = l \times (N/6)^{1/2}$, with l being 0.85 nm in *trans-trans* conformation.
- [37] Note that ultrathin deposits of pure PCL in the same conditions show dendritic structures with about 10 nm-thick crystalline lamellae (unpublished results). See also: V.H. Mareau, R.E. Prud'homme, Macromolecules 38 (2005) 398.
- [38] When tested on several FETs, we observe that bottom-contact FETs show less reproducible properties than top-contact FETs (e.g. some of the output characteristics of bottom-contact FETs display discontinuities in the I–V curves). These differences between the two types of devices likely arise from different interface morphologies at the gold electrodes-semiconducting (co)polymer thin film.
- [39] J.F. Chang, B.Q. Sun, D.W. Breiby, M.M. Nielsen, T.I. Solling, M. Giles, I. McCulloch, H. Sirringhaus, Chem. Mater. 16 (2004) 4772.
- [40] G.M. Wang, J. Swensen, D. Moses, A.J. Heeger, Appl. Phys. 93 (2003) 6137.
- [41] D.M. DeLongchamp, R.J. Kline, E.K. Lin, D.A. Fischer, L.J. Richter, L.A. Lucas, M. Heeney, I. McCulloch, J.E. Northrup, Adv. Mater. 19 (2007) 833.
- [42] I. McCulloch, M. Heeney, M. Chabinc, L.D. DeLongchamp, R.J. Kline, M. Coelle, W. Duffy, D. Fischer, D. Gundlach, B. Hamadani, R. Hamilton, L. Richter, A. Salleo, M. Shkunov, D. Sporrowe, S. Tierney, W. Zhong, Adv. Mater. 21 (2009) 1091.
- [43] (a) R.J. Kline, M.D. McGehee, E.N. Kadnikova, J.S. Liu, J.M.J. Fréchet, Adv. Mater. 15 (2003) 1519;
(b) R.J. Kline, M.D. McGehee, E.N. Kadnikova, J.S. Liu, J.M.J. Fréchet, M.F. Toney, Macromolecules 38 (2005) 3312.
- [44] (a) A. Zen, J. Pflaum, S. Hirschmann, W. Zhuang, F. Jaiser, U. Asawapirom, J.P. Rabe, U. Scherf, D. Neher, Adv. Funct. Mater. 14 (2004) 757;
(b) P. Schilinsky, U. Asawapirom, U. Scherf, M. Biele, C.J. Brabec, Chem. Mater. 17 (2005) 2175.
- [45] J.D. Yuen, R. Menon, N.E. Coates, E.B. Namdas, S. Cho, S.T. Hannahs, D. Moses, A.J. Heeger, Nat. Mater. 8 (2009) 572.